

Formation of dislocation patterns: Computer simulations

R. Fournet and J. M. Salazar*

*Laboratoire de Recherches sur la Réactivité des Solides, UA 23 CNRS, Université de Bourgogne, Faculté des Sciences Mirande,
Boîte Postale 128, 21004 Dijon Cedex, France*

(Received 23 May 1995; revised manuscript received 31 October 1995)

Dislocations patterns have been extensively studied by means of TEM. In parallel, theoretical approaches have been developed by using two methods; reaction diffusion schemes and computer simulation models. This distinction is not rigid since some computer models include the former approach in their evolution equations. Independently from the difficulties each approach presents in formulating the collective behavior of dislocations, the aim of these studies is to exhibit simple dislocation patterns as persistent slip bands and/or cellular organization. In this context, computer simulations brought a methodology which undoubtedly is a complement to the existing approaches for dislocations. Nevertheless, several remarks must be pointed out about the results obtained with the method. First, the conditions of simulations (e.g., cutoff procedure, periodic boundaries conditions), have been extensively criticized and responsible for spurious patterns. Second, the simulations developed do not show clearly the formation of cell structures. Third, the simulations performed do not tell us about the evolution of dislocation patterns in function of the parameters such as dislocation density, external force, or friction stress. The aim of the simulations presented here is to study at the mesoscopic scale the formation of dislocation patterns in two dimensions. For this, we used systems of large dimensions $(20\mu)^2$ and rigid boundaries conditions which permitted us to avoid a cutoff procedure. The simulations performed exhibit the formation of dipolar walls present in persistent slip bands and clearly show the formation of cell organizations. For each pattern observed, we have deduced relationships between the size of the patterns and the parameters used as dislocation density, external force, or friction stress. And indeed, the results obtained show a good agreement with experimental laws.

I. INTRODUCTION

The classical theory of dislocations has permitted one to elucidate the main properties of individual dislocations and to address the difficult question of plastic deformation or strain hardening of metals and alloys.¹⁻⁴ These theoretical studies have been corroborated by experimental results based on transmission electron microscopy (TEM). Beside this, interacting dislocations can present complicated patterns like persistent slip bands (PSB's), labyrinth and/or cell structures for which our knowledge is limited to some interaction mechanisms between dislocations. Thus the theoretical approaches developed until now, for dislocation patterning, are mainly qualitative. This is due to the complexity of the non-linear physical mechanisms intervening during plastic deformation. Moreover, the dislocation patterning presents a dynamical behavior similar to that of physical systems driven far from equilibrium and where spatiotemporal pattern formation is present.

The studies developed by means of TEM have deduced some of the main mechanisms responsible for dislocation patterning, for example, dipole formation, the number of active slip systems, annihilation, and multiplication processes.^{5,6} Moreover, they have permitted one to deduce several scaling laws for the observed patterns relating the flow stress with the dislocation density and with the size of the cells obtained.⁷⁻⁹ These scaling laws can be explained by means of interaction mechanisms between dislocations (e.g., forest mechanisms). But frequently, it is difficult to make a correct interpretation of the experimental results when more than one dislocation mechanism is activated.

Beside the experimental studies, we have theoretical approaches intent on giving an explanation to the observed patterns. For instance, in analogy with the spinodal decomposition of solids, Holt¹⁰ has studied the formation of a cell organization in two dimensions by means of a diffusion equation. The model shows a spontaneous structuration of dislocations without the action of an external force. However, some of the hypotheses made in this model have been contested.⁷ Some of the arguments given against Holt's results are that he did not use a random initial distribution of dislocations (each dislocation was surrounded by dislocations of opposite Burgers vectors) and a cutoff radius of $\rho^{1/2}$ (where ρ corresponds to the dislocation density) was introduced in the calculation of the interaction forces. The latter point facilitates the formation of patterns as has been demonstrated in Refs. 11 and 12. To study theoretically the collective behavior of a density of dislocations some of the methods used are reaction, reaction-diffusion schemes, and computer simulations. In the latter approach some models (cellular automata) include diffusionlike equations (see Ref. 7 and references therein). A pioneer study on the collective behavior of dislocations was developed by Walgraef and Aifantis.^{13(a),13(b)} These authors used a formulation based on the coupling of two partial differential equations expressing the spatiotemporal evolution of mobile and slow dislocations; the description includes local interactions between dislocations, for example, annihilation, multiplication or dipole formation. The motion was assumed to be diffusive and the dynamical analysis showed the formation of dislocation patterns observed experimentally. However, as was pointed out by Shiller and Walgraef^{13(b)} and in Ref. 14 the dependence of

the parameters in function of the stress or the temperature must be improved to facilitate the comparison between the experimental and theoretical results. Moreover, Kratochvil *et al.*¹⁵ have developed a reaction-diffusion model to study the formation of veins and dipolar walls in monocrystals under cyclic loading. This last approach is based on the distinction between two kinds of dislocations: mobiles which are responsible of the plastic deformation and dipoles producing the strain hardening. In this formulation, the diffusive character of dislocations is given in terms of internal stress gradients and the analysis shows that it is possible to observe, qualitatively, the formation of vein structures and PSB's. However, the considerable number of equations in the model limits an analytical stability analysis.

As mentioned above, the study of dislocation patterning by computer simulations has been developed by using mainly cellular automata or molecular dynamics. A great advantage of these methods is that, as the computer models are developed by using the elementary properties of dislocations, we can avoid some drastic approximations on the dislocation interactions used in some analytical models. Among these computer simulations we can find those of Lepinoux *et al.*,¹⁶ who used the notion of cellular automata to study, in two dimensions, the dynamics of a random distribution of edge and screw dislocations. In this formulation, the dislocations are free to move in their glide plane and in a perpendicular direction associated to the climb mechanism, local interactions (e.g., annihilation and multiplication of dislocations) and periodic boundaries conditions were used. The simulations show several interesting features like the possibility to obtain the formation of dipolar walls. Moreover, they show that it is impossible to obtain a spontaneous dislocation structure without the action of an external force. Another computer simulation approach, using the basis of molecular dynamics, was developed by Amodeo and Ghoniem.¹⁷ Their work was centered on the study of the formation of PSB's and cellular structures in two dimensions. For this, they considered a simulation cell with a random distribution of edge dislocations obeying their local interactions mechanisms (i.e., annihilation, multiplication, dipoles formation.). In this approach, the dislocation motion is determined by the action of an external force and the elastic interaction between dislocations. The results obtained, when only one glide system is activated, show the formation of a dislocation wall at the center of the simulation cell and when two glide systems are activated a fairly clear cell organization is observed.

Most of the computer simulations described above were performed for systems of small size ($\approx 1\mu^2$) with periodic boundaries conditions and where the range of interaction was limited to half the size of the simulation box. It is important to remark that these last restrictions imply, as was stated by Gulluoglu *et al.*,¹¹ that it is possible to obtain spurious patterns, for instance, polygonization walls which appear when the dislocation density is very high.¹² Until now, the only studies in three dimensions are those developed by Kubin *et al.*,^{18–20} to study at the mesoscopic scale the plastic deformation in a single crystal. Their approach is based on a discretization of a dislocation loop into edge and screw segments. Each segment can interact with each other and the multiplication process is taken into account. By this method it is possible to quantify at the mesoscopic scale the plastic

deformation in relation with the dislocation theory. For the moment, the deformation produced cannot exceed one percent due to the complexity of interactions introduced in the model.

The studies we present here were focused to clarify some of the difficulties encountered in dislocation patterning, namely, the formation of dipolar walls and cellular organization. Our computer simulations were developed at the mesoscopic scale for a single crystal of copper of $(20\mu)^2$ under cyclic loading and under rigid boundary conditions. The plan of the paper is as follows. In Sec. II, we briefly explain the dislocation physics used in the algorithm and we calculate the forces exerted on each dislocation. In Sec. III, we develop the algorithm used. In Sec. IV, we give relevant numerical results when one or two glide systems are activated and we derive the resulting relationships. In Sec. V, we summarize the main results obtained in our study.

II. DISLOCATION THEORY AND MOLECULAR DYNAMICS

Nowadays, molecular dynamics is a powerful tool in the study of solid state problems. The methodology used is particularly adapted to dislocation problems. Indeed, dislocations can be considered as elementary elements which move under the action of forces. Hence it is possible to study, at mesoscopic scale, the spatiotemporal evolution of a given dislocation distribution in function of the forces exerted on these point defects. These long range forces can be separated in three processes: interactions between dislocations, interaction between dislocations and an external stress field, and interaction between dislocation and the crystal lattice. Moreover, dislocations are line defects which can interact between each other at short distance. Then, it is necessary to introduce in the formulation local interactions like annihilation or multiplication.

A. Long range interaction forces

It is well known that the presence of a dislocation in a crystal produces a deformation field which can be divided in two parts: a plastic deformation near the core of the dislocation and an elastic one where the linear theory of elasticity can be applied. If we suppose that the core of a dislocation can be approximated by an incompressible area, then the stress field produced by an edge dislocation can be considered as an elastic stress. In this case, we can use the equations for plane deformation which are satisfied by any solution of the biharmonic equation²¹

$$\nabla^4 \chi = 0, \quad (1)$$

and where the elastic stress field in cylindrical coordinates can be written as

$$\sigma_{rr} = \frac{1}{r} \frac{\partial \chi}{\partial r} + \frac{1}{r^2} \frac{\partial^2 \chi}{\partial \theta^2}, \quad (2a)$$

$$\sigma_{\theta\theta} = \frac{\partial^2 \chi}{\partial r^2}, \quad (2b)$$

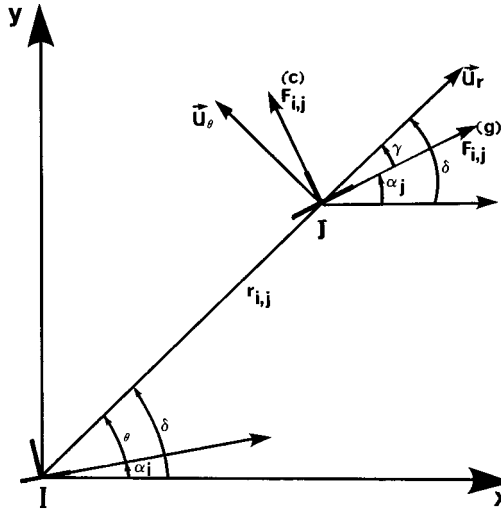


FIG. 1. Referential frame related to the interaction forces between two edge dislocations.

$$\sigma_{r\theta} = -\frac{\partial}{\partial r} \left(\frac{1}{r} \frac{\partial \chi}{\partial \theta} \right). \quad (2c)$$

To obtain a solution for the last equations, we can use functions of the form

$$\chi = R(r)\Theta(\theta), \quad (3)$$

and solve the resulting ordinary differential equations for r . In this way, a solution for a positive edge dislocation is of the form

$$\chi = -\frac{\mu b}{2\pi(1-\nu)} r \ln r \sin \theta, \quad (4)$$

where μ is the shear modulus, ν is the Poisson's ratio, b is the norm of the Burgers vectors, and θ is the angle between the Burgers vector and the direction ij (see Fig. 1). Then, the elastic stress field in cylindrical coordinates is given by

$$\|\sigma_{i,j}\| = \frac{\mu b}{2\pi(1-\nu)r_{ij}} \begin{pmatrix} -\sin \theta & \cos \theta & 0 \\ \cos \theta & -\sin \theta & 0 \\ 0 & 0 & -2\nu \sin \theta \end{pmatrix}. \quad (5)$$

The force exerted on the dislocation i by the dislocation j is calculated by means of the Peach-Koelher relation²²

$$\vec{F}_{ij} = (\vec{b}_i \overline{\sigma_{ij}}) \times \vec{L}_j. \quad (6)$$

Given that in the z direction the dislocation j is parallel to the dislocation i , the forces to be considered are in the (r, θ) plane (see Fig. 1). Hence the forces expressed on the referential frame of the dislocation j are

$$\vec{F}_{ij}(r, \theta) = \frac{k}{r_{ij}} \begin{pmatrix} \cos \theta \cos(2\gamma) \\ \sin \theta + \sin(2\gamma) \cos \theta \end{pmatrix} = \begin{pmatrix} F_{ij}^g \\ F_{ij}^c \end{pmatrix}, \quad (7)$$

where F_{ij}^g, F_{ij}^c are respectively the glide and the climb components of the j dislocation. The latter component is activated at high temperatures and is related to the diffusion of point defects.¹

In general, studies on plastic deformation are associated with the presence of an external force which can be monotonous or cyclic.^{5,6} Here, we used a cyclic external loading and the resulting forces were calculated by using Eq. (6). Hence, if the external stress field is given by σ_{ext} , its corresponding force on a dislocation i can be expressed as

$$\vec{F}_{\text{ext}} = (\vec{b}_i \overline{\sigma_{\text{ext}}}) \times \vec{L}_i. \quad (8)$$

Another force acting on a dislocation is the friction force, F_{friction} , which gives us a lower bound of the external force to be applied on a dislocation to set its movement on a glide plane. The friction stress is always opposite to the motion of the dislocations and its origin can be related to several factors, for instance, the action of the crystal lattice, the presence of impurities, or the influence of other dislocations. For cubic face centered metals the value of the friction force is relatively low ($10^{-5}\mu$) and for cubic centered metals or covalent structures this value is higher.²³

B. Local interactions

Dislocations can interact between each other at short range implying complex atomic rearrangements on the crystal.¹⁻⁴ These interactions have been detailed by remarkable experimental studies^{5,6} where we can find the conditions under which they appear. The dislocation processes most frequently used^{13(a),13(b),16,19} for studying dislocation patterning are annihilation, multiplication, and pinning of dislocations. The annihilation process corresponds to the destruction of two dislocations of opposite Burgers vectors approaching each other within a critical region. The critical distance between these two defects is, in the case of an edge dislocation in Cu, approximately equal to 1.6 nm.²⁴ This process, which is activated at high temperature, induces the well-known recovery process in strong hardened metals.²¹ The multiplication of dislocations is a complex process responsible of the strain hardening in materials, and a well known mechanism is the Frank-Read source.⁴ This process can be schematically described as follows: under the action of a shear stress, σ , a pinned line of dislocation can be bent. If this stress is sufficiently high, the curvature of the line passes through a maximum forming a semicircle which evolves, under the action of σ , into a complete dislocation loop containing in its interior the initial line of dislocations. If the applied stress exceeds this value, the line can increase beyond a semicircle and become a complete loop and restore the initial line of dislocation. This mechanism produces a large number of dislocation loops under the action of relatively small stress (μb^2). During plastic deformation, the dislocation density increases considerably and some of the created dislocations become immobile. The pinning of dislocations creates a forest of dislocations which interacts with mobile dislocations. If a dislocation passes through the forest it may form jogs or junctions resulting from the local interactions between the dislocations and the forest.²

C. Equation of motion

The next step consists in deriving an equation of motion for each dislocation in function of the forces described above. Each edge dislocation can move on a slip plane parallel to its Burgers vector and in a perpendicular direction (i.e., the climb mechanism). In this case, the equation of motion for an edge dislocation can be written as

$$\vec{F}_i = m_i \frac{d^2 \vec{r}_i}{dt^2}, \quad (9a)$$

with

$$\vec{F}_i = \sum_j \vec{F}_{ij}^{\text{int}} + \vec{F}_{\text{ext}} - \vec{F}_{\text{friction}}. \quad (9b)$$

and where $m_i = 1$. Here we assumed that the inertial effects induced by the linear mass of the dislocations can be neglected since they are nonsignificant.²⁵ Moreover, when the dislocation velocities are smaller than the speed of sound it is possible to express the equation of motion, Eq. (9a), as

$$\vec{v}_i = \frac{\vec{F}_i}{B}, \quad (10)$$

where B corresponds to a damping coefficient ($B = 5 \times 10^{-5}$ Pa s for copper and $B = 5 \times 10^{-4}$ Pa s for aluminium²⁰). This formulation of the equation of motion, in contrast with Eq. (9a) permitted us to use a higher temporal mesh point (10^{-9} s) and lower densities of dislocations.

III. DESCRIPTION OF THE FORMULATION

The formulation, developed here, uses the basis of molecular dynamics and consists in studying the formation of dislocation patterns in two dimensions at the mesoscopic scale. Several points differentiate our approach from classical problems of molecular dynamics. First, the forces used do not derive from an interaction potential. Secondly, the elastic interaction between two dislocations is a function of the angle between their two Burgers vectors [see Eq. (7)]. This angular dependence introduces an anisotropy in the elastic interaction force and increases the difficulty to calculate it. Thirdly, dislocations are line defects which can interact at short distance. In consequence, we must take into account within the dynamical evolution of the dislocation distribution several processes like annihilation or multiplication. Here, the system is constituted of an ensemble of parallel edge dislocations disposed randomly inside a simulation cell. The numerical procedure consists in calculating for each dislocation its new position and velocity resulting from the forces acting on it. This is done in two steps: First, we calculate the new velocity for each dislocation by using the equation

$$v_i(t+dt) = \frac{F_i(t)}{B}, \quad (11)$$

where F_i corresponds to the total force exerted on a dislocation i and defined by Eq. (9b), and secondly by using Eq. (11), we determine the dislocation positions given by

$$r_i(t+dt) = r_i(t) + dt v_i(t), \quad (12)$$

where dt corresponds to the time step used. In a two-dimensional approach, it is nearly impossible to formulate correctly both the forest mechanisms and the multiplication process. To overcome this difficulty we introduced in the system a sufficiently high dislocation density. Moreover, the procedure we used to simulate the annihilation process was as follows: for any couple of dislocations i, j we checked both if their Burgers vectors were parallel or antiparallel and if the distance separating the dislocations, $r_{i,j}$, was greater or smaller than the critical annihilation distance r_a . Then, if the Burgers vectors were antiparallel and if $r_{ij} < r_a$, the dislocations i and j were annihilated. To maintain a dislocation velocity smaller than a critical velocity, v_c (usually the speed of sound), it is necessary to perform a scaling of the velocities. This consists in supposing that the total kinetic energy of the dislocations is constant in time. In this case, we obtain a Gaussian distribution of velocities for the dislocations around an average velocity v_0 .²⁶ The scaling of velocities is performed by using a scaling factor β given by

$$\beta = \left[\frac{(2N-3)k_b T_{\text{ref}}}{\sum_i v_i^2} \right]^{1/2}, \quad (13)$$

where $(2N-3)$ are the degrees of freedom, k_b is the Boltzmann constant, T_{ref} is a temperature reference for the system, and v_i is the velocity of the dislocation i . By multiplying β by the velocity [Eq. (11)], we can determine the new distribution of velocities, that is,

$$v_{i+1} \leftarrow \beta v_{i+1}. \quad (14)$$

The scaling is performed if more than 20% of the density of dislocations have a velocity greater than 100 m/s or smaller than -100 m/s corresponding approximately to 100-iterations steps. To be thorough, we calculated the elastic interaction energy between dislocations which for edge dislocations is given by

$$W_{ij}^{\text{int}}(r_{ij}, \theta_i) = -\frac{\mu b_i b_j}{2\pi(1-\nu)} \ln \frac{r_{ij}}{r_0} + \frac{\mu b_i b_j}{2\pi(1-\nu)} \cos(2\theta_i + \alpha), \quad (15)$$

where $\alpha = \alpha_i - \alpha_j$ and $r_0 \approx b$ (region of the dislocation core). It is clear that the temporal evolution of the elastic interaction energy does not characterize the formation of a dislocation pattern but it is useful to verify that the system evolves towards a configuration of equilibrium.

IV. SIMULATIONS AND NUMERICAL RESULTS

A. Simulations

We performed computer simulations for a distribution of edge dislocation in two dimensions by using the procedure described in the last section. To avoid a cutoff procedure we used systems of large dimensions $(20\mu)^2$ and rigid boundary conditions, that is, any dislocation arriving at the boundary of the simulation cell cannot leave it (zero flux), but it can move to the interior of the cell if this movement leads to a dislocation configuration that minimizes the elastic energy. At the beginning of the simulation we introduced a random configuration of dislocations ranging from 300 to 1000 which corresponds approximately to a density of about 10^{12}

TABLE I. Constant parameters used in the simulations.

Metal	Burgers vector (nm)	Poisson ratio	Shear modulus (GPa)	Time step (s)
Copper	2.5	0.324	42	10^{-9}

cm^{-2} . The time step used was equal to 10^{-9} s and was deduced from the mean free path of a dislocation which varies like $\rho^{-1/2}$. For a dislocation density of 10^{12} cm^{-2} the mean free path is equal to 1μ . If we suppose that the mean velocity for the dislocation is $\approx 1 \text{ m s}^{-1}$ this implies that the characteristic time, dt , is equal to 10^{-7} s. Then, a fraction of one percent of this time represents a good estimation of the time step needed in a simulation. In our simulations the time step was assumed to be constant in contrast with Ref. 17 where dt varied considerably ($dt \in [10^{-9} \text{ s}, 1 \text{ s}]$) and which can introduce a divergence problem. At the beginning of the simulations, the velocity of the dislocations and the external force were set equal to zero and the forces created by the dislocation i due to the presence of the remaining $N-1$ dislocations were calculated by using Eq. (7). An external force has been applied on the system in the glide direction of the dislocations. The procedure which permits us to calculate this last force can be explained as follows: we considered a constant stress tensor,

$$\sigma_{i,j}^{\text{ext}} = \begin{pmatrix} 0 & \sigma_{1,2} \\ \sigma_{1,2} & 0 \end{pmatrix},$$

acting on the system and corresponding to an experimental shear stress used in the study of patterns like persistent slip bands. The application of this external stress induced on each dislocation a force which can be calculated by using Eq. (6). Then, for a dislocation i of Burgers vector $b_i = (b_i^x, b_i^y)$ the force is equal to

$$\vec{F}_{\text{ext}} = \begin{pmatrix} b_i^x \sigma_{1,2} \\ b_i^y \sigma_{1,2} \end{pmatrix};$$

this external forcing was applied in the glide direction each 500 iteration steps. This periodicity, deduced numerically, corresponds to the time necessary for a complete relaxation of the system and does not correspond to the frequency experimentally used (1 Hz). Due to the low deformation obtained at the end of each simulation ($\epsilon^{\text{tot}} < 1\%$) we neglected the rotation effect associated to the action of the shear stress.

The numerical procedure detailed in the last paragraph was used when either one or two slip systems were activated. In the former case, we were interested in the formation of dipolar walls while in the latter case we studied the formation of cellular structures. In both cases, we analyzed the influence of the dislocation density, the external force, and the friction stress on the resulting patterns. In Table I are given the constants used during the simulations.

B. Dipolar walls

In this subsection, we report the results obtained when only one glide system was activated (Fig. 2). Figure 3(c) shows the resulting configuration obtained after 10^4 iteration

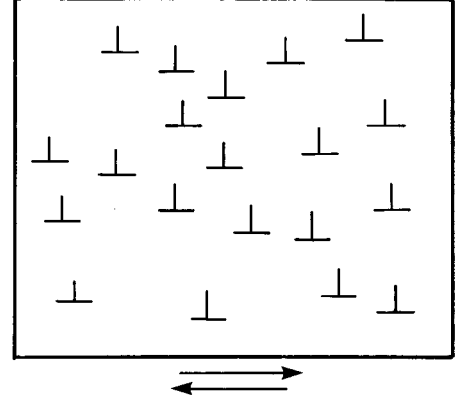


FIG. 2. Active slip system associated to the formation of dipolar walls.

steps for a system of $(20\mu)^2$ containing 550 dislocations ($\rho = 1.37510^{12} \text{ m}^{-2}$) and for a friction stress of about 0.36 MPa. Identical results were obtained for different densities of dislocations and in all the cases we did not observe a spontaneous structuration. In contrast, when we applied a cyclic stress of ± 3 MPa, we obtained the formation of four dipolar walls [Fig. 4(b)]. A common feature to these simulations is the decrease of the elastic interaction energy towards a stable configuration [Figs. 3(b) and 4(c)]. The oscillations on the energy shown in Fig. 4(c) correspond to the effect of the cyclic external force which is responsible for the inversion of polarity in the walls. Moreover, in these simulations the an-

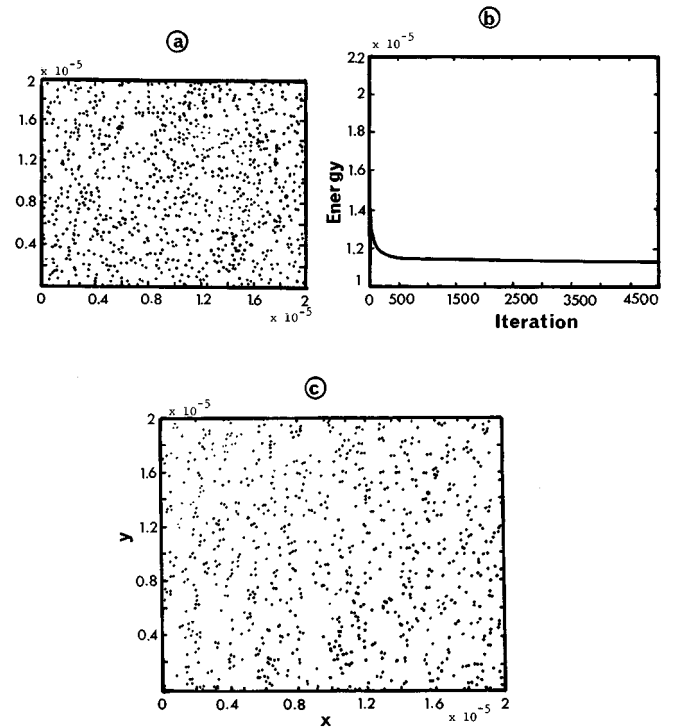


FIG. 3. Configuration obtained for a square area of $(20\mu)^2$ containing a density of $1.37510^{12} \text{ m}^{-2}$ without an external force. (a) Initial configuration of dislocations. (b) Evolution of the elastic energy of the system (J m^{-1}). (c) Configuration obtained after 5000 iteration steps.

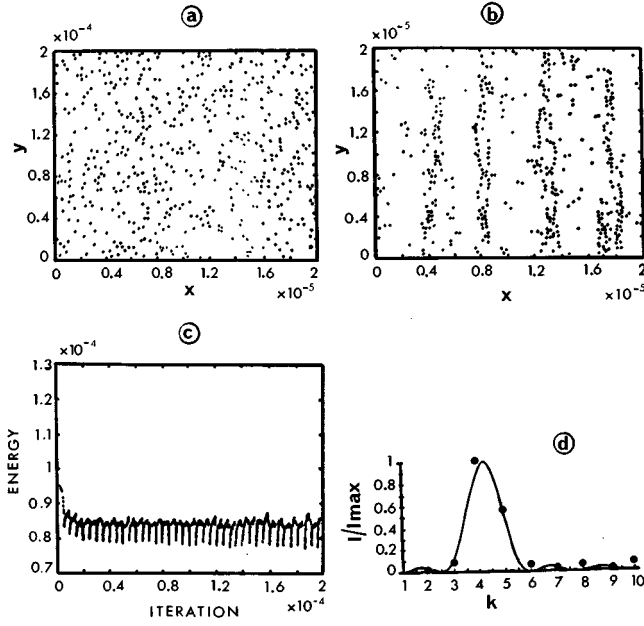


FIG. 4. Dipolar walls obtained for a square area of $(20\mu)^2$ containing a density of $1.37510^{12} \text{ m}^{-2}$ when a cyclic external force of 0.36 MPa was applied. (a) Initial configuration of dislocations. (b) Configuration obtained after 15000 iteration steps. (c) Evolution of the elastic energy of the system (J m^{-1}). (d) Fourier transform obtained from (b).

nihilation effect is almost negligible due to the low dislocation density. In all the simulations performed less than one percent of the dislocations were annihilated. Figure 5 gives the velocity distribution of dislocations after 1000 iteration steps and shows that the major part of the dislocations have a velocity lower than $[30] \text{ m s}^{-1}$. This last verifies our hypothesis concerning the mean velocity used in the calculation of the time step. The spatial organizations obtained [Fig. 4(b)] are in agreement with those given by Devincere²⁰ and demonstrate that we cannot obtain a dislocation pattern with a single slip system and without an external stress. To char-

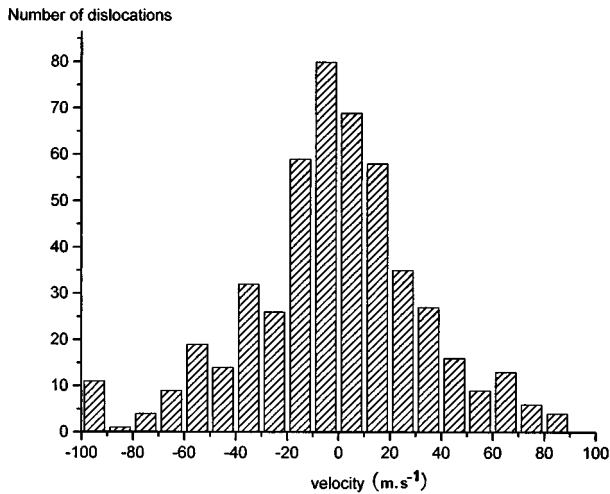


FIG. 5. Example of a velocity distribution during a simulation.

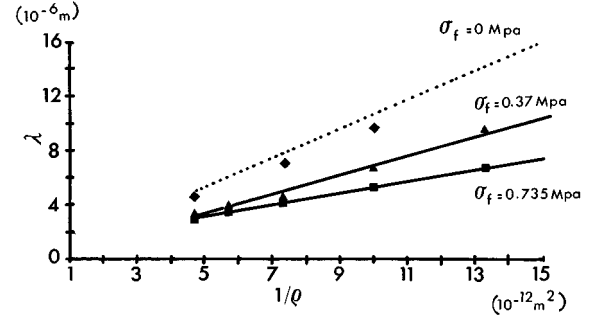


FIG. 6. Variation of λ with the inverse of the dislocation density and the friction stress. The dashed line was calculated by using Eq. (12) and the value of k used is given in Ref. 20.

acterize the obtained patterns we performed a Fourier transform of the resulting density distribution of dislocations. This was done in the following way: we divided the x axis of the simulation box into equally spaced mesh points (20 mesh points) and then we counted the dislocations lying in each interval. This last gives us the local distribution in function of the space to which we fitted a curve. And subsequently, we performed the Fourier transform to the fitted curve. The deduced characteristic length, λ , is in fact an average value of several Fourier transforms and its accuracy is of $\pm 0.2\mu$. This allowed us to deduce a scaling behavior characteristic to each observed pattern. The power spectrum of Fig. 4(d) gives a maximum with a period equal to $k=4.3$. Hence the wavelength is given by

$$\lambda = \frac{n\Delta x}{k} = 4.75 \mu\text{m},$$

where $\Delta x = 1\mu$ and $n=20$ correspond respectively to the distance between mesh points in the x direction and to the total number of mesh points. For different values of Δx ranging from 0.01 to 1.0 the results converge. Moreover, we studied the influence of the dislocation density and the friction force on the characteristic length of dipolar walls. Figure 6 recapitulates the results obtained and shows the evolution of λ in function of the inverse of the dislocation density. The three curves presented correspond to three different values of the friction stress F_{friction} . The dashed and solid lines correspond to the results obtained in Ref. 20 whereas the points below were determined by our simulations. Each point in the curves corresponds to the average value of several simulations and we can see that λ decreases as the dislocation density increases. This behavior can be represented by the following scaling:

$$\lambda = \frac{k}{\rho}, \quad (16)$$

where k is a constant parameter calculated in Ref. 20 for a zero friction stress and given by

$$k = \frac{16\pi(1-\nu)\tau}{\mu b}, \quad (17)$$

where τ equals the effective stress.

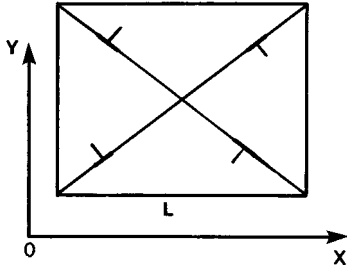


FIG. 7. Active slip system associated to the cell formation.

The formation of dipolar walls can be explained and interpreted as follows: an initial stage, characterized by the formation of isolated dipoles, occurs in the system. These dipoles are destabilized under the action of the external force and a correlation between dislocations of the same sign appears leading to the formation of subgrain boundaries. Then, opposite subgrains can assemble to form a dipolar wall.

We analyzed the influence of the F_{friction} on the characteristic length. In this case, we obtained that λ decreases as F_{friction} increases. This result can be explained in the following way: each dipolar wall formed during a simulation creates a stress field which leads to push the other walls. When $F_{\text{friction}}=0$, the motion of a dislocation is easier and the space between two walls is maximal and fixed by the dislocation density. However, when $F_{\text{friction}} \neq 0$, the range of the stress field created by a wall is shorter and the mobility of the dipolar walls decreases. In consequence, λ cannot be maximal. An extreme case occurs (i.e., nonformation of dipolar walls) for values of friction stress greater than 1.26 MPa.

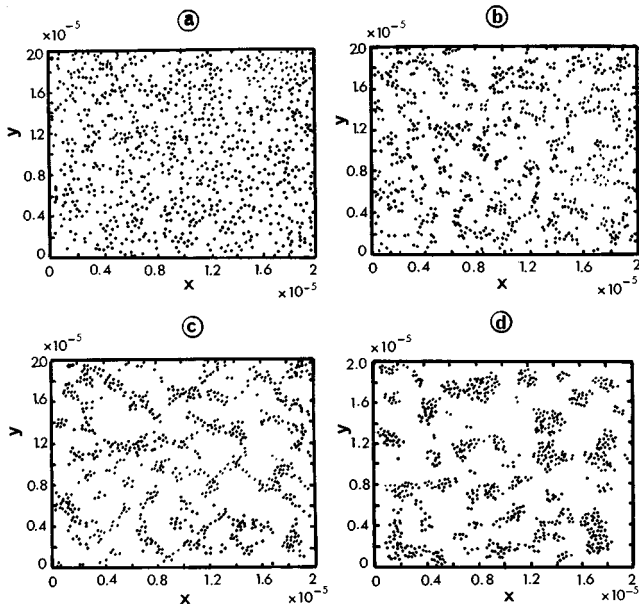


FIG. 8. Cell organization obtained for a square area of $(20\mu)^2$ containing a dislocation density of $2.510^{12} \text{ m}^{-2}$. (a) Initial configuration of dislocations. (b) Configuration obtained after 200 iteration steps without external force. (c) Configuration obtained after 1000 iteration steps without external force. (d) Configuration obtained after 1000 iteration steps with $\sigma/\mu=10^{-3}$.

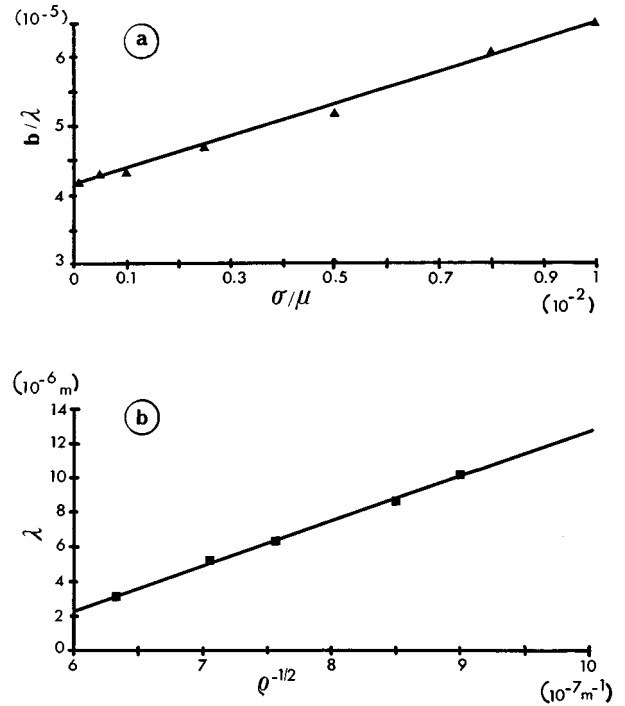


FIG. 9. Variation of λ with the inverse of the external applied (a) and the inverse of the square root of the dislocation density (b).

C. Cellular organization

The conditions under which a cellular organization appears differ completely from those to observe dipolar walls. In the latter case, only one active slip system is necessary to observe the formation of walls perpendicular to the glide direction, while in the former case we require the activation of a secondary slip system. Another possibility, which facilitates the formation of cellular structures consists to increase the temperature in order to activate the climb process. Here, we focused our attention on studying the formation of dislocation cells, starting from a random distribution of dislocations and by considering two slip systems parallel to the diagonals of the simulation box (Fig. 7). Moreover, we considered the climb process in the determination of the elastic interaction forces [see Eq. (7)] and the constants used during the simulations are given in Table I. Figure 8(c) gives a typical configuration obtained for a dislocation density of $2.510^{12} \text{ m}^{-2}$ without an external force and with a $F_{\text{friction}}=4.2 \text{ MPa}$. The last figure shows clearly the formation of a cell organization after 1000 iterations where the structuration starts to develop by the formation of clusters composed of “pseudodipoles” uniformly distributed in space [Fig. 8(b)]. And afterwards, mobile dislocations join these clusters to give a cellular organization. Figure 8(d) gives the configuration obtained in the same conditions as those of Fig. 8(c) with an applied stress equal to $\rho/\mu=10^{-3}$. Figure 9(a) shows the variation of λ in function of the applied stress. In fact, we have represented these parameters in reduced coordinates: b/λ for the cell size and ρ/μ for the external stress. Each point in Fig. 9(a) corresponds to a mean

value of the characteristic length calculated in the x and y directions by means of a Fourier transform. For $\sigma \neq 0$, it is easy to show that the relation between λ and the inverse of the applied stress can be approximated by the following relation:

$$\frac{\rho}{\mu} = k \frac{b}{\lambda}, \quad (18)$$

where b is the norm of the Burgers vectors, μ is the shear modulus, and $k=20$ is a constant which was assimilated during a long time with an universal constant.⁷ In our studies $k \geq 400$. Figure 9(b) shows the evolution of λ in function of the inverse of the square root of the dislocation density with a constant external force ($\rho/\mu = 10^{-2}$). The results reported in the last figure allow us to write

$$\lambda \propto \rho^{-1/2}. \quad (19)$$

This evolution is in agreement with those reported in Refs. 7–9.

V. CONCLUSIONS

In this paper, we analyzed the formation of dislocation patterns by using concepts emerging from molecular dynamics. The computer simulations reported permitted us to clarify several questions of dislocation patterning.

(a) The formation of dipolar walls when only one slip system is activated requires necessarily the application of an external force [Fig. 4(b)].

(b) The results in Fig. 6 allow us to qualitatively describe the evolution of the dipolar walls in function of the dislocation density and the friction force as $\lambda = k/\rho$. Moreover, our computer experiments suggest that the main parameters responsible for the formation of dipolar walls are the external force and the long range interaction forces.

(c) The results obtained when two active slip systems and the climb process are activated show that it is possible to observe the formation of a cell organization [Fig. 8(c)] and the Fourier analysis of these cell structures allowed us to write two scaling relationships:

$$\frac{\rho}{\mu} = k \frac{b}{\lambda} \quad \text{and} \quad \lambda \propto \rho^{-1/2},$$

which are in excellent agreement with the experimental results reported in Ref. 7

ACKNOWLEDGMENTS

We thank Professeur L. P. Kubin for his helpful discussions. The simulations were supported by IDRIS-CNRS, France.

*Electronic address: jmarcos@satie.u-bourgogne.fr

¹J. Friedel, *Dislocations* (Pergamon, New York, 1964).

²A. H. Cottrell, *Dislocations and Plastic Flow in Crystals* (Clarendon, Oxford, 1953).

³F. R. Nabarro, *Theory of Crystal Dislocations*, International Series of Monographs on Physics (Clarendon, Oxford, 1967).

⁴W. T. Read, *Dislocations in Crystals* (Wiley, New York, 1953).

⁵C. Laird, P. Charsley, and H. Mughrabi, *Mater. Sci. Eng.* **81**, 433 (1986).

⁶F. Ackermann, L. P. Kubin, J. Lepinoux, and H. Mughrabi, *Acta Metall.* **32**, 715 (1984).

⁷L. P. Kubin, in *Treatise in Materials Science and Technology*, edited by R. Cahn, P. Haasen, and E. J. Kramer (VCH, Weinheim, 1993), Vol. 6, Chap. 4, pp. 137–187.

⁸S. J. Basinski and Z. S. Basinski, in *Dislocation in Solids*, edited by F. R. N. Nabarro (North-Holland, Amsterdam, 1979), Vol. 4, pp. 261–362.

⁹S. V. Raj and G. M. Pharr, *Mater. Sci. Eng.* **81**, 217 (1986).

¹⁰D. L. Holt, *J. Appl. Phys.* **41**, 3197 (1970).

¹¹A. N. Gulluoglu, D. J. Srolovitz, R. LeSar, and P. S. Lomdahl, *Scr. Metall.* **23**, 1347 (1989).

¹²J. M. Salazar and R. Fournet, *Solid State Phenom.* **35–36**, 613 (1994).

¹³(a) D. Walgraef and E. C. Aifantis, *Int. J. Eng. Sci.* **23**, 1351 (1985); (b) C. Shiller and D. Walgraef, *Acta Metall. Mater.* **36**, 563 (1988).

¹⁴J. M. Salazar, R. Fournet, and N. Banai, *Acta Metall. Mater.* **43**, 1127 (1995).

¹⁵J. Kratochvil, in *Basic Mechanisms in Fatigue of Metals*, edited by P. Lukas and J. Polak (Elsevier, Prague Academia, 1988), pp. 15–25.

¹⁶J. Lepinoux, *Solid State Phenom.* **3**, 335 (1988).

¹⁷R. J. Amodeo, and N. M. Ghoniem, *Phys. Rev. B.* **41**, 6958 (1990).

¹⁸L. P. Kubin *et al.*, in *Non Linear Phenomena in Materials Science II*, edited by G. Martin and L. Kubin (Trans Tech, CH-Aedermannsdorf, 1992), p. 445.

¹⁹B. Devincere and M. Condat, *Acta. Metall. Mater.* **40**, 2629 (1992).

²⁰B. Devincere, Thèse de doctorat, Paris XI Orsay, 1993.

²¹A. H. Cottrell, *Theory of Crystals Dislocations* (Gordon and Breach, New York, 1964).

²²M. Peach and J. S. Koehler, *Phys. Rev.* **40**, 436 (1950).

²³H. Neuhuser, O. B. Arkan, and H. H. Potthoff, *Mater. Sci. Eng.* **81**, 201 (1986).

²⁴U. Essmann and H. Mughrabi, *Philos. Mag.* **40**, 731 (1979).

²⁵J. Weertman and J. R. Weertman, in *Dislocations in Solids*, edited by F. R. N. Nabarro (North-Holland, Amsterdam, 1980), Vol. 4, Chap. 8, pp. 1–61.

²⁶D. W. Heermann, *Computer Simulation Methods* (Springer-Verlag, New York, 1986).